1. Faiçal KHARCHOUCHE[1], 2. Abdelkrim ZEBAR[2]

DAC-hr Laboratory, Electrical Engineering Department, University of Ferhat Abbas Setif 1, Setif 19000, Algeria (1)
QUERE laboratory, Electrical Engineering Department, University of Ferhat Abbas Setif 1, Setif 19000, Algeria (2)
ORCID: 1.   0000-0003-2306-6806; 2. 0009-0005-6087-3641

Effect of Fe$_2$O$_3$ doping on the electrical and microstructural properties of ZnO-(Bi2O3, Sb2O3) varistor ceramics

Abstract. This study will allow us to see the effect of Fe$_2$O$_3$ doping on the electrical and microstructural properties of the ceramic varistor based on (Bi$_2$O$_3$, Sb$_2$O$_3$). The study deals with a ZnO-based varistor, containing, 0.5 mol% of (Bi$_2$O$_3$, Sb$_2$O$_3$) doped with 1 mol%, 2 mol%, and 4 mol% of Fe$_2$O$_3$. The ceramics samples were developed using the conventional route of the oxides mixture, sintered all the samples at 1000 °C. The mean grain size increased with the increase of the Fe$_2$O$_3$ amount and the grains were homogeneous, the varistors exhibited the relative density, the dielectric constant (ε'), dielectric dissipation factor (tanδ) and leakage current (IL) was increased with the increase of the Fe$_2$O$_3$ amount, Therefore, the nonlinearity coefficient (α) decreases from 23.58 to 8.61 and the breakdown field (Eb$_{1mA}$) decreased from 341.41 to 202.01V/mm with an increase in the amount of Fe$_2$O$_3$.

*Streszczenie. Badania te pozwolą nam zobaczyć wpływ domieszkowania Fe$_2$O$_3$ na właściwości elektryczne i mikrostrukturalne warystora ceramicznego na bazie (Bi$_2$O$_3$, Sb$_2$O$_3$). Badania dotyczyły warystora na bazie ZnO, zawierającego 0,5% mol (Bi$_2$O$_3$, Sb$_2$O$_3$) domieszkowanego 1% mol, 2% mol i 4% mol Fe$_2$O$_3$. Próbki ceramiki opracowano konwencjonalną drogą mieszaniny tlenków, wszystkie próbki spiekano w temperaturze 1000°C. Wraz ze wzrostem zawartości Fe$_2$O$_3$ zwiększała się średnia wielkość ziaren i ziarna były jednorodne, warystory wykazywały gęstość względną, wraz ze wzrostem zwiększała się stała dielektryczna (ε'), współczynnik rozproszenia dielektrycznego (tanδ) i prąd upływu (IL). ilości Fe2O3, zatem współczynnik nieliniowości (α) maleje z 23,58 do 8,61, a pole przebicia (Eb1mA) zmniejsza się z 341,41 do 202,01V/mm wraz ze wzrostem ilości Fe$_2$O$_3$. (**Wpływ domieszkowania Fe2O3 na właściwości elektryczne i mikrostrukturalne ceramiki warystorowej ZnO-(Bi2O3, Sb2O3**)*

Keywords: Varistor; Fe$_2$O$_3$ doped- ZnO; Dielectric properties; Electrical properties.
Słowa kluczowe: warystor; domieszkowany Fe$_2$O$_3$ – ZnO; Właściwości dielektryczne; Właściwości elektryczne.

Introduction

Varistors are electrical elements that have variable resistivities depending on the electric field which is used for protection against overvoltages, allowing to avoid the propagation of these electrical disturbances in a system (e.g. electrical network or electronic circuit): mounted in parallel with the circuit to be protected, this type of component allows limiting the effect of overvoltages without impacting the operation of the system to be protected [1, 2]. The main characteristic of varistors is their variable electrical conductivity, depending on the voltage applied to their terminals: very insulating at low voltage, varistors become very conductive above their transition voltage, called "threshold voltage". The extraordinary physical and chemical properties of zinc oxide have made it the providential candidate that can bring a significant improvement in the quality of many components, and even more so improve the varistor effect [1-3]. ZnO has already been tested with microcrystalline materials and has given some satisfaction; it has a variable resistance and a high coefficient of nonlinearity as well as a low loss under operating voltage. Many zinc oxide-based varistors on the market are used as lightning arresters [3, 4]. This is formed at about 98% by moles of ZnO. The remaining 2% corresponds to additives. The choice of the optimal chemical compositions leads to the development of varistors having a high non-linearity coefficient resulting essentially from empirical work that requires quantities of experimental plans. The addition of oxides metal results in an influence on the electrical characteristics and/or on the microstructure of the final material developed during production or shaping. We give in the following paragraphs the main constituents encountered in the varistors through the effects they have on the properties of the material and the role they play in their elaboration. The conditions for the enhancement of varistors based on ZnO have in particular the subject of much research to lead to the implementation of manufacturing processes optimal. The addition of cobalt and manganese decreases the interstitial zinc concentration in the zinc oxide; this decrease leads to the number of donor defects, therefore of the density of charge carriers and thus decreases the conductivity [4, 5]. Varistors in this day exhibit high non-linear current-voltage characteristics. They are the most time-consuming produced by sintering a mixture of ZnO powders considered as a matrix with weak quantities of other types of metal oxides like SnO$_2$, Bi$_2$O$_3$, TiO$_2$, SrTiO$_3$, BaTiO$_3$, Sb$_2$O$_3$, WO$_3$ or even CeO$_2$ [4-9]. The choice of these oxides is their wide bandgap semiconductor character (Eg > 3 eV). The nonlinear current-voltage electrical characteristic of ceramic zinc oxide-based varistors is due to the formation of double Schottky barriers at the grain boundaries. Preparation of commercial ZnO-Bi$_2$O$_3$ varistors by the classical method. However, this method is not easy to control with high precision, resulting in desirable grain microstructure and electrical characteristics. For this, several studies have been set up to know the effect of certain dopants like Ce$_2$O$_3$, Ho$_2$O$_3$, La$_2$O$_3$, Dy$_2$O$_3$, Y$_2$O$_3$, etc., in particular on the increase in grain size or the control of the microstructure of ZnO-based varistors as well as the electrical characteristics [7-14]. Varistor formulations the most common contain bismuth and antimony oxides; these form with zinc oxide, the spinel Zn$_7$Sb$_2$O$_{12}$ and pyrochlore Bi$_3$Zn$_2$Sb$_3$O$_{14}$ phases as well as several bismuth-rich phases. These phases are generally located in the intergranular zones. Zinc oxide-based varistors exhibit semiconductor and nonlinear properties.

(1) $$I = K V^\alpha$$

where α represents the non-linearity coefficient of conduction. There are many nonlinear systems such as SiC, SrTiO$_3$, TiO$_2$, WO$_3$, etc [2, 3, 8, 11-14]. These materials have nonlinearity coefficients that are always weak and are therefore unsuitable for electrotechnical applications such as medium voltage surge arresters, on the other hand, they can be used for protection against overvoltages in low voltage [1, 3, 13]. We have thus prepared for the first time varistors based on zinc oxide

"Sb$_2$O$_3$ /Bi$_2$O$_3$/ZnO" doped with Fe$_2$O$_3$. The samples thus obtained go through a series of characterizations to highlight the quality of the finished product. For the study of the electrical properties of the ZnO-based varistors we used a device equipped with a nano-ammeter (Keithley 237, measure source unit), we also took into consideration the electrical properties and Several analyzes were used for the morphological and structural identification such as: scanning electron microscopy (SEM) to ensure the homogeneity and conformity of the chemical composition of the samples.

Experimental procedure

In the case of this study, we chose a high-purity nano-ZnO powder (Nanogard, 99.99% purity, average particle size 60 nm). Standard proportions of additives such as Bi$_2$O$_3$ and Sb$_2$O$_3$ powder have been incorporated with zinc oxide powder as shown in this formula of 99% ZnO + 0.5% Bi$_2$O$_3$ + 0.5% Sb$_2$O$_3$ (all in mol%). Subsequently, pure powdered Fe$_2$O$_3$ (1, 2 and 4 mol%) was used in the preparation of four samples, where the basic composition was the following system 99% ZnO + 0.5% Bi$_2$O$_3$ + 0.5% Sb$_2$O$_3$+Xmol% Fe$_2$O$_3$ (ZBS+ Xmol% Fe$_2$O$_3$). The formula for each sample is abbreviated as follows Z0 (ZBS), Z1 (ZBS+ 01mol% Fe$_2$O$_3$), Z2 (ZBS+ 02mol% Fe$_2$O$_3$) and Z3 (ZBS+ 04mol% Fe$_2$O$_3$), the experimental protocol for the elaboration of our varistors has been made by the classic way of mixing oxide. Selected powders are mixed in small amounts (~50g), in deionized water with zirconia beads and ethanol, in polypropylene vials filled with 5 mm diameter zirconia beads, using a mixer. The mixing time is about 2 hours. The balls promote the homogenization of the mixture but are not there for the purpose of grinding the powders. The low rotation speeds (2 rev/min) also avoid pollution of the mixture by any debris from zirconia beads. The powders are then dried in an oven at 110° C. for 12 hours. The powders then undergo calcination carried out in a superkhantal Linn air oven with isothermal maintenance at 800°C for 2 hours (rise ramp of 10°C.min-1). However, the recovered powder mixture is ground in a mortar and sieved through a 200 µm sieve. Shaping by pressing requires the powder to have a certain cohesion allowing it to be obtained from compact discs pressed from 0.5 g of powder. For this, we added to the powder an organic binder based on a mixture of polyvinyl alcohols (PVA), diluted in an aqueous medium at 4% by weight which promotes the raw mechanical strength of the pressed samples. The binder coats the grains to form a thin plastic layer which leads to the formation of so-called 'soft' easily deformable agglomerates which help the arrangement of the particles during pressing. The incorporation is done in a porcelain mortar at the rate of two drops for a batch of 10g of powder so as to have a paste. The latter is dried at 80°C in an oven for one hour then recovered, crushed in a mortar and sieved through a 200µm sieve. Our technique consists of getting in shape the initial powder. Two complementary compression protocols were implemented: uniaxial compression (on a Sodemi RD20E press equipped with a cylindrical die) at sufficient pressure to ensure the cohesion of the compact, followed by cold isostatic compression at higher pressure (Cold isostatic press, 4000bar, 15x15x20, Novassis). Maximum pressure of 40 MPa is reached with uniaxial pressing. Beyond this pressure, the samples are cracked. The isostatic pressure reached is 300 MPa for 5 min. This type of forming generally makes it possible to reach relative densities when raw (before sintering) of the order of 60 to 70% of the theoretical density of the material. The dimensions of the cylindrical compacts prepared by pressing are close to 8mm in diameter and 1.5mm thick.

Sintering was performed at 1000°C for 2 h with a heating and cooling rate of 5°C/min in a programmable oven for all samples. The Archimedes method was applied to determine the density of the samples. In order to highlight and understand the microstructural modifications induced by densification, and to have better control of the microstructural evolutions to optimize the electrical and dielectric properties, the four samples were characterized by high-resolution scanning electron microscopy and mapping. EDX (Hitachi S-3500N). The grain size was measured based on the intercepted segment method (linear interception) [4, 5, 15]. The principle of this method consists in tracing several segments of length L on the micrograph to be characterized and in counting the number N of grains intercepted. Grains not fully cut are counted as half a grain. In order to ensure better contact with the electrodes (measuring device), the pellets are metalized using a thin layer of silver paste on both sides of the pellet, followed by annealing, in an oven. conventional, at 650°C for 10 min. The diameter size of the electrodes was 8 mm. The size of the electrodes was 8 mm in diameter. The parameters Eb, JL and α could then be determined from the current/voltage characteristic obtained using a voltage source equipped with a nano-ammeter (Keithley 237, measure source unit). By convention, we define the non-linearity coefficient α,

$$(2) \qquad \alpha = \frac{(Log J2 - Log J1)}{(Log E2 - Log E1)}.$$

With J$_1$ and J$_2$ equal to 1 mA.cm^{-2} and 10 mA.cm^{-2} respectively. Graphically, it corresponds to the slope of the log J = f (log E) representation. As part of this work, we were interested in some of these parameters, in particular, the dielectric constant ε', the loss factor ε'' and the loss tangent tanδ were measured using an impedance analyzer type HP4194A. Also, the dielectric constant can be calculated by this equation.

$$(3) \qquad \varepsilon r = \frac{c}{c_v}.$$

where C is the capacity of the material under test and Cv is the capacity of air. In an alternating electric field, the complex dielectric permittivity given by this formula is shown.

$$(4) \qquad \varepsilon = \varepsilon'(\omega) - j\varepsilon''(\omega).$$

Where ε' is the dielectric constant, ε'' is the dielectric loss factor. The tangent of the loss angle is called the dielectric dissipation factor. It is given by the following relation [13, 16].

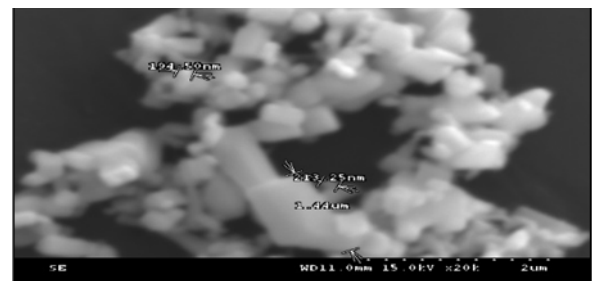$$(5) \qquad tan\delta = \frac{\varepsilon''}{\varepsilon'}.$$

Fig.1. SEM image of ZnO powder.

Results and discussion

The observation of the surface or the morphology of zinc oxide powders by scanning electron microscopy SEM allows both to verify the grain size and the shape of the grains. The ZnO powders obtained are characterized by

SEM and the corresponding images are shown in Fig.1, a similar morphology, consisting of large aggregates agglomerated between them. These aggregates are made up of nanoparticles and microparticles. As well as we allowed viewing that the particle size of ZnO varies from 100 nm to 1.5 µm.

So, the analysis that was carried out by EDX makes it possible to determine the composition and distribution of the chemical elements in our analyzed sample (Bi_2O_3, Sb_2O_3)-doped ZnO-based varistor sintered at 1000°C for two hours containing 4mol% Fe_2O_3 (Fig 2). According to the mode used in this work, we were able to perform an elemental analysis at a specific point (on a volume of approximately 5µm). The results of the EDS (Fig.2,b) analysis presented the elemental compositions with a high concentration of additives such as Fe, Zn, Bi, Sb and O. it is clear that the distribution of the chemical elements is well dispersed in a homogeneous way for each component. EDX mapping of the elemental distribution shows that Fe is highly dispersed in the ZnO matrix.
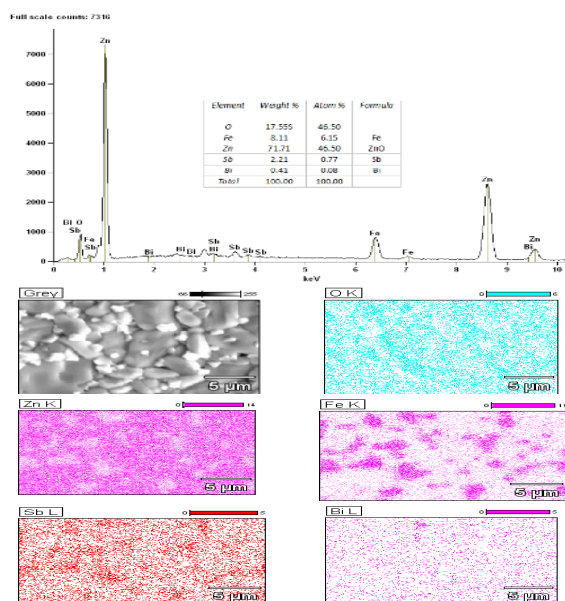

Fig.2. EDX spectrum and EDX mapping of the elemental distribution of Zn, O, Sb, Bi and Fe of (Bi_2O_3, Sb_2O_3)-doped ZnO based varistor sintered at 1000°C for two hours containing 4mol% Fe_2O_3.

After the sintering step, all samples that are used in the studies presented here are from the same batch in an oven programmable for two hours at a temperature of 1000 ∘C, the sintered samples were characterized by SEM on fracture facies in order to study the evolution of the microstructure according to the effect of the Fe_2O_3 dopant. we can see the morphology of all the samples through the SEM, Fig.3, presenting the fracture images, highlights a distribution of grains homogeneous in size and shape. However, significant differences appear between all the samples. Relative to the average grain size of ZnO. This is more frankly shown in the data in Table 1 which gives the particle size of ZnO. we see that the smallest grain size corresponds to the sample (Z0). We see on the micrographs of the four samples that there is a decrease in the ZnO grain restricted by the introduction of Fe_2O_3, and the grain size increases from 2.88 µm to 5.34 µm. In addition, the grains appear more tightly " welded " throughout the sample. The growth in grain size can be accounted for by the precipitation of the second phase in grain boundaries and nodal points. The shape and size of

the Z0 sample particles were different. The bimodal microstructure of the large and fine grains of the matrix was well illustrated in the Z0 sample. The evolution of the grain size of the samples is noted in Table 1. The Z0 sample seems more porous compared to the other Fe_2O_3 doped sample. Fe_2O_3 in moles as a dopant improves grain size and improves microstructure uniformity. in general. Microstructural analysis by SEM shows that the samples have fine and coarse grains similar to that of the Z0 sample with other bright fine grains). The SEM images show that the more the Fe_2O_3 content is incorporated, the more the porosity of the sample is reduced. the density of the samples – measured by the Archimedes method – is between 5.60 and 5.64, i.e. 97.2 to 98.15% of the theoretical density. Almost complete densification is therefore obtained for all the experiments carried out.
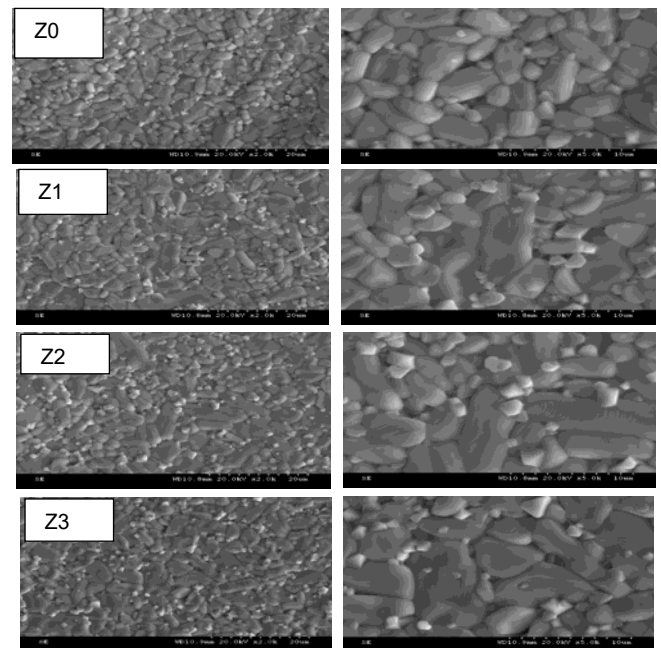

Fig.3. SEM micrographs of (Bi_2O_3, Sb_2O_3)-doped ZnO based varistors and sintered at 1000 °C containing various amounts of Fe_2O_3.

J–E characteristic behavior, of the elaborated varistors, is displayed in Fig.4. The breakdown voltage decreases from 341.41 to 202.01 when Fe_2O_3 increases from 0 to 4 mol% Fe_2O_3 with a firing temperature of 1000°C. Hence, Fe2O3 has a big influence on the breakdown, grain size and grain boundaries at 1000 °C as indicated in Table 1. The coefficient of nonlinearity (α) follows the behavior of the breakdown field in the function of Fe_2O_3 content and firing temperature. It is observed that the addition of the Fe_2O_3 content decreases the coefficient of nonlinearity.
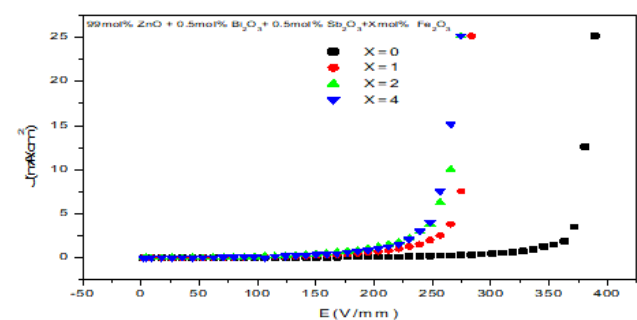

Fig.4. J-E characteristic for 1000°C as sintering temperature.

When increasing Fe_2O_3 contents between 0mol% and 4mol%, the threshold voltage obtained is found to be less than that of the varistor without the addition of Fe_2O_3, it is concluded that the threshold voltage decreases from the addition of the content in Fe_2O_3. The curves confirm that the electrical conduction characteristics share two areas. In the first part of the curve and before, the breakdown field, the current does not almost flow, as a function of the field. In the second part of the curve, after the breakdown field, the current abruptly increases with the increasing electric field. On the whole, the voltage-current relation is nonlinear. The sharpest is the knee of the curves between the two areas whereas it determines the non-linearity coefficient α, Greater is α, the better is the non-linearity of the varistor. The coefficient (α) of the varistor Z0 (without Fe_2O_3) is only 23.58, whereas the values (α) of the samples (Z1, Z2 and Z3) are in the range of 9.4 – 8.61.

Table 1. Summary of all sample data, average ZnO grain size, electrical and dielectric parameters.

Composition	Eb_{1mA} (V mm^{-1})	Eb_{10mA} (V mm^{-1})	α	J_l (mA cm^{-2})	Grain size (µm)	Relative density (%)	ε (1KHz)	ε (10KHz)	tanδ (10KHz)
Z0	341.41	380	23.58	0.269	2.88	97.2	1667	1449	0.154
Z1	221.42	279.51	9.40	0.406	3.94	98.00	2661	2127	0.212
Z2	193.46	265.02	9.20	0.445	4.68	98.2	3202	2534	0.234
Z3	202.01	262.55	8.61	0.415	5.34	98.15	2752	2208	0.227

The electrical and dielectric data are presented in detail in Table 1. The breakdown field (Eb_{1mA}) decreased from 341.41 to 202.01V/mm with an increase in the amount of Fe_2O_3. The behavior of Eb_{1mA} with an increase in the amount of Fe_2O_3 can be explicated by this the relation of Eb_{1mA} is given by this expression.

(6) $$Eb_{1mA} = \frac{V_{gb}}{d}$$

Where d is the average grain size and V_{gb} is the breakdown voltage per grain boundary [4, 7]. When there is an increase in the size of grain growth this will lead to a decrease in the number of grain boundaries. This obviously leads to lower Eb_{1mA}, in the case of tangential lines in the breakdown area. The comportment of the system showed the diminutions of the coefficient of nonlinearity ($α$) from 23.58 to 8.61 with an increase in the quantity of Fe_2O_3 up to 4mol%. This system exhibits a decreased non-linearity. When we add the amount of Fe_2O_3, the decreasing trend of the value is believed to be attributed to the reduction in the height of the potential barrier due to the abrupt difference of the electronic state at the grain boundaries. in another way, it is found that the comportment of leakage current density (J_L) fluctuates with the increasing quantity of Fe_2O_3.

The investigation of the dielectric characteristics for the four varistors produced at a temperature of 1000°C is presented in Fig.5. For the first view, we note that the four varistors have the same evolution of the dielectric constant (ε') and the dissipation factor dielectric (tanδ) as a function of frequency. It is also noted that the varistor Z0 without the addition of Fe_2O_3, shows that the dielectric constant (ε') is low compared to the three other varistors doped with Fe_2O_3. For all samples the ε' decreased with increasing frequency, this decrease is shared between a rapid decrease we can concede it as a relatively strong dispersive drop in the 10 kHz range and another slow decrease above the 200kHz value as a somewhat low dispersive drop, this is attributed to the decrease in the number of conduction carriers, which may follow the test frequency in the dielectric bias. Investigational results showed that the dielectric constant increased with an increase in the quantity of Fe_2O_3. It is clear that this is attributed to the increase in the grain size and the decrease in the depletion layer width, as defined according to the following expression.

(7) $$\varepsilon^r = \varepsilon_{ZnO}\left(\frac{d}{t}\right)$$

Where is ε_{ZnO} the dielectric constant of ZnO (8.5), d is the average grain size, and t is the depletion layer width of both sides at the grain boundaries [4, 5]. The dielectric constant at 1 kHz increased from 1667 to 2752 with an increase in the amount of Fe_2O_3. moreover, the tanδ increased abruptly until the vicinity of 1 kHz, increasing frequency for all samples. moreover, the tanδ increased abruptly until the vicinity of 30 kHz, increasing frequency for all samples. That exhibits a quite high dielectric absorption peak beyond 200 kHz, The tanδ was investigated to have fluctuation with the increase in the amount of Fe_2O_3. The tanδ results from the heating loss by the Joule effect by leakage current and also from the heating loss by friction by rotation of the electric dipole. It is assumed that the reason why all the samples possess a high tanδ is attributed to a rather high leakage current. The more precise dielectric characteristic data are summarized in Table 1

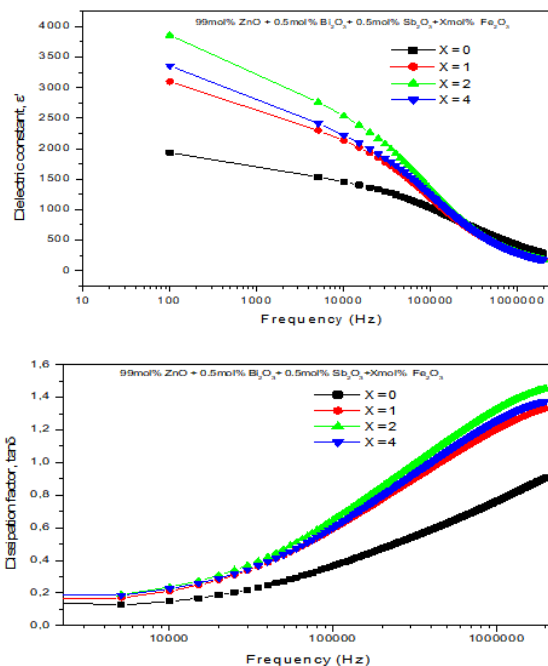Fig.5. Dielectric characteristics of the four samples for different amounts of Fe_2O_3.

Conclusion

Influence of Fe_2O_3 on (Bi_2O_3, Sb_2O_3)-doped ZnO based varistor, has been elaborated using the conventional route. Fe_2O_3 has been added in the range of 1 to 4 mol%. In this work, 1000°C was the choice as sintering temperature. The results are summarized as follows.

The SEM images. The EDX spectrum reveals a high concentration of additives such as Fe, Zn, Bi, Sb and O. EDX mapping of elemental distribution shows that Fe is highly dispersed in the ZnO matrix

The grain size of the samples increases significantly, from 2.88 to 5.34μm, with increasing Fe_2O_3 concentration.

The relative density, the dielectric constant ε', the dissipation factor ($\tan\delta$), and the leakage current density I_L increase with increasing Fe_2O_3 concentration. However, the reverse, non-linearity coefficient (α) and breakdown field (E_b) were decreased, since the grains size increased.

Acknowledgment

Authors: *Faiçal KHARCHOUCHE, DAC-hr Laboratory, Electrical Engineering Department, University of Ferhat Abbas Setif 1, Setif 19000, Algeria, E-mail: faical.kharchouche@univ-setif.dz; Abdelkrim ZEBAR. QUERE laboratory, Electrical Engineering Department, University of Ferhat Abbas Setif 1, Setif 19000, Algeria, E-mail: karimzebar@univ-setif.dz.*

REFERENCES

1. Tonkoshkur A.S., Glot A.B., Ivanchenko A.V., Percolation effects in dc degradation of ZnO varistors, *Adv. J. Dielect,* 05 (2015), **No. 01, 1550008**
2. *Kharchouche F., microstructure and electrical properties of $CaCO_3$-doped ZnO– (Bi_2O_3, Sb_2O_3) based varistor ceramics.* Rev. Roum. Sci. *Techn.–Électrotechn. et Énerg.*67(2022), No.1, 439–444
3. Etienne S., Sylvain M., Franck G., Yoshiaki K., Julien P., Richard R., Peculiar effects of microwave sintering on ZnO based varistors properties, *J. Alloys Compd*, 50 (2011) 96163–6169,
4. Kharchouche F., Effect of sintering temperature on microstructure and electrical properties of ZnO-0.5 mol%V_2O_5-0.5 mol%Cr_2O_3 varistors, *J. Mater. Sci.: Mater. Electron,* 29 (2018), 3891–3897
5. Szwagierczak D., Kulawik J., SKkwarek A., Influence of processing on microstructure and electrical characteristics of multilayer varistors, *J. Adv. Ceram.* 8(2019), No. 3, 408–417
6. Bernik S., Macek S., Bui A., Microstructural and electrical characteristics of Y_2O_3-doped ZnO–Bi_2O_3-based varistor ceramics, *J. of the European Ceramic Society,* 21(2001), No.10, 1875–1878
7. ŁOWK B., ZIAJA J., KRAFT A. A., The influence of the electrode material on the dielectric properties of PET films, *Przeglad Elektrotechniczny*, 99 (2023), No. 1, 58-61
8. Tominc S., Rečnik A., Bernik S., Mazaj M., Spreitzer M., Daneu N., Microstructure development in (Co,Ta)-doped SnO_2-based ceramics with promising varistor and dielectric properties, *J. Eur. Ceram. Soc.* 40 (2020), No. 15, 5518-5522
9. Peng P., Deng Y., Niu J., Shi L., Xu D, Fabrication and electrical characteristics of flash-sintered SiO_2-doped ZnO-Bi_2O_3-MnO_2 varistors, *J. Adv. Ceram,* 9 (2020),683–692.
10. Hu G., Zhu J., Yang H., Wang F., Effect of CuO addition on the microstructure and electrical properties of SnO_2-based varistor, *J. Mater. Sci: Mater Electron.* 24 (2013), 2944–2949
11. Billovits, T., Kaufmann, B., Supancic, P., Measurement of the piezotronic effect on single grain boundaries in zinc oxide Varistors. *Open Ceramics*, 6 (2021), 100125
12. Matsuoka M., Masuyama T., Iida Y., Voltage nonlinearity of Zinc oxide ceramics doped with alkali earth metal oxide, Japanese, *Journal of Applied Physics*, 8 (1969), No.10, 1275–1276
13. Ahmed Z.W., Khadim A.I., Alsarraf A.H.R., The effect of doping with some rare earth oxides on electrical features of ZnO varistor, *Energy Procedia*, 157 (2019) 909–917
14. Mei L.T., Hsiang H.I., Hsi C.S., Yen F.S., Na_2CO_3 doping effect on ZnO-Pr_6O_{11}-Co_3O_4 ceramic varistor properties, *J. of Alloys and Compounds*, 558 (2013), 84–90
15. Sendi R.K., Fabrication of high voltage gradient ZnO nanoparticle-Bi_2O_3-Mn_2O_3-based thick film varistors at various sintering temperature, *Journal of King Saud University-Science.* 34 (2022), No. 3, 101820
16. Wang Z., Li W., Chu R.Q., Hao J.G., Xu Z.J., Li G., Structure and piezoelectric properties of $(Ba_{1-x}Ca_x)(Ti_{0.95}Hf_{0.05})O_3$ lead−free ceramics, *Mater Res Bull*, 97 (2018), 334-342